



Simultaneous appraisals of pathway and probable health risk associated with trace metals contamination in groundwater from Barapukuria coal basin, Bangladesh



Md Ahsan Habib ^a, Abu Reza Md Towfiqul Islam ^{b,*}, Md Bodrud-Doza ^c, Farhana Afroj Mukta ^b, Rahat Khan ^d, Md Abu Bakar Siddique ^e, Khampheng Phoungthong ^f, Kuaanan Techato ^a

^a Faculty of Environmental Management, Prince of Songkla University, Songkhla, 90112, Thailand

^b Department of Disaster Management, Begum Rokeya University, Rangpur, 5400, Bangladesh

^c Climate Change Programme, BRAC, Dhaka, 1212, Bangladesh

^d Institute of Nuclear Science & Technology, Bangladesh Atomic Energy Commission, Savar, Dhaka, 1349, Bangladesh

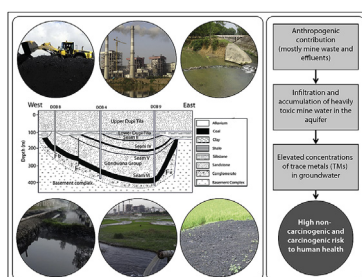
^e Institute of National Analytical Research and Service (INARS), Bangladesh Council of Scientific and Industrial Research (BCSIR), Dhaka, 1205, Bangladesh

^f Environmental Assessment and Technology for Hazardous Waste Management Research Center, Faculty of Environmental Management, Prince of Songkla University, Songkhla, 90112, Thailand

HIGHLIGHTS

- Groundwater pathways and associated health risks were appraised in the Barapukuria coal basin.
- Leaching of coal effluences and anthropogenic inputs are the main causes for groundwater pollution.
- Pb, Cd and Cr are the most hazardous pollutants of the groundwater in the coal basin.
- Chromium was the predominant contaminant and its carcinogenic risk cannot be ignored.
- The most sensitive parameter of potential risk was C and EF for adult and IR for children.

GRAPHICAL ABSTRACT



ARTICLE INFO

Article history:

Received 7 April 2019

Received in revised form

6 October 2019

Accepted 20 October 2019

Available online 23 October 2019

Handling Editor: Martine Leermakers

Keywords:

Groundwater resources

Trace metals

Health risk appraisal

ABSTRACT

In this study, we analyzed 33 groundwater samples from the Barapukuria coal basin (BCB), Bangladesh for 10 trace metals (TMs) using Atomic Absorption Spectroscopy. Pathways and associated probable health risk were appraised by employing multivariate statistical approaches, health risk model and Monte-Carlo simulation. Except for the Cu, Cr and Zn concentrations, the mean concentrations of all TMs in the basin were above the permissible water quality limits set by Bangladesh and international standards. Correlation coefficient and principal component analysis, supported by cluster analysis indicated that anthropogenic inputs were more contributed to the elevated concentrations of TMs compared to geogenic sources as the major reasons of groundwater pollution in the basin. The results of non-carcinogenic risk appraisal depicted that hazard index (HI) values for both adults and children were exceeded the safe limits (>1.0) except for few locations, indicating serious health risks on the human via oral and dermal absorption pathways. However, the carcinogenic risk values of Cd and Cr exceeded the

* Corresponding author.

E-mail address: towfiq_dm@brur.ac.bd (A.R.M.T. Islam).

Barapukuria coal basin
Monte-Carlo simulation

US EPA range of 1×10^{-6} to 1×10^{-4} , with higher risk for children than adults, with oral intake as the key exposure pathway. A sensitivity study identified the concentration of Cr, exposure frequency and ingestion rate for carcinogenic effect as the most sensitive parameters influencing the probable health risk. Overall, the results suggest that Cr in drinking water could cause detrimental effects to exposed local residents; thus, strict health regulation and groundwater management should concentrate on Cr contamination in groundwater from the coal basin.

© 2019 Elsevier Ltd. All rights reserved.

1. Introduction

Natural processes (e.g., leaching and weathering) and anthropogenic inputs (e.g., mining and industrial activities) with increased utilization of groundwater resources during urbanization widely affect water quality (Galhardi and Bonotto, 2017; Islam et al., 2017a). Poor water quality has drawn worldwide attention due to increasing dependence on groundwater for securing the quality of life (Sengupta and Agrahari, 2017). Globally, more than 880 million people lack safe drinking water, with about 2.6 billion people having little or no sanitation, and millions of people die every year from water-borne diseases associated with contaminated groundwater (Kibria et al., 2016). Groundwater pollution is mostly related to man-made activities, and trace metals (TMs) contamination has become a global concern due to the high persistence, toxicity and carcinogenicity of such metals in humans and other ecosystems (Voltaggio et al., 2015; Sengupta and Agrahari, 2017). In recent time, the elevated concentrations of TMs are continuously releasing in surrounding environments and consequently these TMs seepage into groundwater, which poses serious health risks to human via different exposure pathways (Kumar et al., 2017; Qiu et al., 2018; Islam et al., 2017b; Singh et al., 2018; Ahmed et al., 2019). Thus, basic appraisals of the pathways, sources, contamination level, and probable health risk associated with TMs in groundwater resources are necessary to control pollution and effective water management plans.

Coal mining and combustion activities play an important role for growing economies and for the progress of developing countries like Bangladesh, and China and the production and combustion of fuel coal have dramatically increased in recent decades (Singh et al., 2018; Habib et al., 2018, 2019). Inherently, coals and associated residuals are mainly composed of, among other substances, naturally occurring substances such as incombustible organic matter, different toxic TMs, carcinogenic polyaromatic hydrocarbons (PAHs), and minute amounts of radionuclides (Islam et al., 2011), which are released from the coal matrix in gaseous, solid and liquid forms to the ambient environment (Ito et al., 2006). However, there are a number of environmental issues associated with coal mining, processing, conversion and combustion (Prasad and Kumari, 2008). Various types of mine wastes and their residues are generated due to coal burning, and subsequently these wastes may enter into soils and followed by groundwater, potentially contributing to contamination (Bhuiyan et al., 2010; Halim et al., 2013). Coal mining, and combustion residuals in ash ponds generally affect both the hydrogeology and groundwater quality (Zeng et al., 2018). Because of coal mine activities, groundwater contamination is an acute problem around the globe (Ochieng et al., 2015). A number of studies reported that coal mine impacts include mine drainage system, subsidence of land, poorer water levels and severe water shortage in adjacent areas, flow path change of groundwater, and contamination of exploitable aquifers because of infiltrated poor-quality mine water (Newman et al., 2017; Zaman et al., 2018). In addition, coal waste adds different toxic TMs such as Cd, Cu, Cr, Pb, Ni, As and Zn which may release into water bodies and form the most serious prolonged hazards for groundwater (Finkelman et al.,

2018). These TMs have been extensively implicated in human health risk and diseases (Sengupta and Agrahari, 2017). In fact, the quantification of the level of TMs to human through different exposure pathways is vital (Islam et al., 2015). Thus, a health risk appraisal model is employed to assess the probable human health risks of under groundwater contaminants by calculating the probability of undesirable impacts in health (Geng et al., 2016; Lu et al., 2015; Fallahzadeh et al., 2017). A number of recent studies have applied the health risk appraisal model to assess the severe impacts of TMs to humans in many countries (Zeng et al., 2018; Rahman et al., 2018; He et al., 2018; Ahmed et al., 2019; Islam et al., 2019).

The Barapukuria coal basin (BCB) is the only active coal basin in Bangladesh which is located in Dinajpur shield (Howladar and Islam, 2016). This basin is currently facing several water-related problems (Zaman et al., 2018). First, acid mine drainage (AMD) occurs in the coal basin due to the weathering of sulfide-rich mine waste and consequently, it can create elevated concentrations of TMs which enter into the groundwater system through natural leaching process (Silva et al., 2013; Galhardi and Bonotto, 2017). Second, the inappropriate disposal of mine waste and combustion byproducts could expose to ambient environment, and can finally access the aquifer, resulting in water pollution (Halim et al., 2013). Third, the entire basin is littered with big piles of coal waste, and flying coal-dust and combustion residuals (Habib et al., 2018). The mine drainage water that comes out of the pits dug inside the mine carries coal-dust and subsequently, contributes to leaching of contaminants from soil to groundwater systems (Jelic et al., 2017). These can cause groundwater TMs pollution which has become more severe in the basin under the background of rapid urbanization and economic growth (Zaman et al., 2018).

Studies from worldwide coal basin, e.g., Tshikondeni coal basin, South Africa (Nephelama and Muzerengi, 2016), Linhuan coal basin, China (Qiu et al., 2018), Korba coal basin, India (Singh et al., 2017), Thrace coal basin, Turkey (Erarslan et al., 2014), Mugla coal basin, Turkey (Baba et al., 2003), and the Bokaro coal basin, India (Tiwari et al., 2017) have stated that the groundwater of these basins is highly polluted with TMs. Several attempts have been carried out on TMs contamination in groundwater resulting from coal mining and burning activities in Bangladesh (Bhuiyan et al., 2010; Halim et al., 2013; Hossain et al., 2015; Khan et al., 2017). Bhuiyan et al. (2010) stated that the elevated contents of TMs Such as Pb, Mn, and As in water bodies were found in the proximal part of the basin. Halim et al. (2013) showed the migration and impact of elevated TMs in water of the BCB area. These studies clearly point out that coal basin area enormously affects the quality and quantity of groundwater. However, previous studies of TMs have only concentrated on the combination of mine water, surface water, soil, and fly ash (Bhuiyan et al., 2010; Hossain et al., 2015; Khan et al., 2017) and also have very limited dataset of groundwater samples which cannot provide the actual scenarios of TMs pollution. Systematic investigations of TMs source, pathways, distributions, and associated with potential health risk in the BCB are still lacking. This is the first attempt of its nature being performed on probable human health risk in the BCB. The objectives of the research are to: i) determine the concentrations and pathways of TMs in the

groundwater samples from the BCB, with comparison to drinking water quality in Bangladesh and to international standards; ii) identify the potential sources of the TMs using multivariate statistical approaches; and ii) appraise probable health risk of TMs in local inhabitants using health risk model and Monte-Carlo simulation. These outcomes provide a scientific background for managing groundwater and protecting human health based on water resources in the Barapukuria basin.

2. Experimental and methodology

2.1. Site description

The Barapukuria coal basin (BCB) is located at Parbatipur and Phulbari sub-districts (an administrative part), Dinajpur, Bangladesh (Fig. 1) with an area of about 6.68 km². Demographically, this area is moderately to densely populated (density: 823/km²) with multi-cropped agricultural land. Geomorphologically, the area is situated at the northern fringe of a Pleistocene terrace named the level Barind Tract and in humid subtropical region in alluvial-fluvial floodplain system. The area is crossed by a number of streams associated with the Khorkhori, Jamuna and Ghirnai rivers. Groundwater is the only source for local drinking and irrigation water purposes. The average annual precipitation in the area is 1800 to 2000 mm, of which 85% comes in the rainy season (May to September). The mean annual temperature is 26 °C and the relative humidity ranges between 50% (winter season) and 85% (rainy season).

Geologically, the BCB is located in the Dinajpur Shield of Bangladesh. The basin is blanketed mainly with unconsolidated Holocene Tista alluvial fan sediments and the Pleistocene Barind clay, which were developed under fluvial-alluvial and rapidly

prograding deltaic conditions. The Pleistocene sediments are underlined by the Plio-Pleistocene Dupi Tila formation (Islam and Hayashi, 2008). Considering the hydro-geologic setting of this BCB, it is noted that this basin belongs to a more complex hydro-geological system than other basins in Bangladesh. The aquifer occurs within the Upper Dupi Tila sand formation underlying the Barind clay. The aquifer constitutes the major water resources in the basin having average thickness of about 104 m. The Upper Dupi Tila sand formation is known as shallow aquifer which encompasses a number of aquifers comprising of dominantly unconsolidated fine to medium-grained sandstones, pebbly sandstones and clay/mudstone, claystone composition (Islam and Hayashi, 2008). The hydraulic gradients, average transmissivity, permeability, storage coefficient and specific yield values of aquifer are 0.0004–0.0006, 12,000 m²/day, 0.004 and 25–30%, respectively (Howladar and Islam, 2016). Aquifers are semi-confined to confine in nature. The groundwater recharge occurs mostly from heavy rainfall and local river waters during the rainy season, resulting in the lateral flow from the southwestern part of the BCB. This basin is known as coal mine under water, because of the presence of thick aquifer over the coal seam layers, where groundwater flows from NE to SW direction having almost flat hydraulic gradient and vertical flow is more significant compared to horizontal flow (Majumder and Shimada, 2016).

2.2. Sample collection and analysis

Groundwater samples were randomly sampled from 33 sites surrounding the Barapukuria coal-fired power plant (BCPP) and coal mine in Barapukuria basin area from March–May 2017, with well pumping from the depth of about 20–50 m (Fig. 1). The March–May is usually dry month in Bangladesh. The consumption

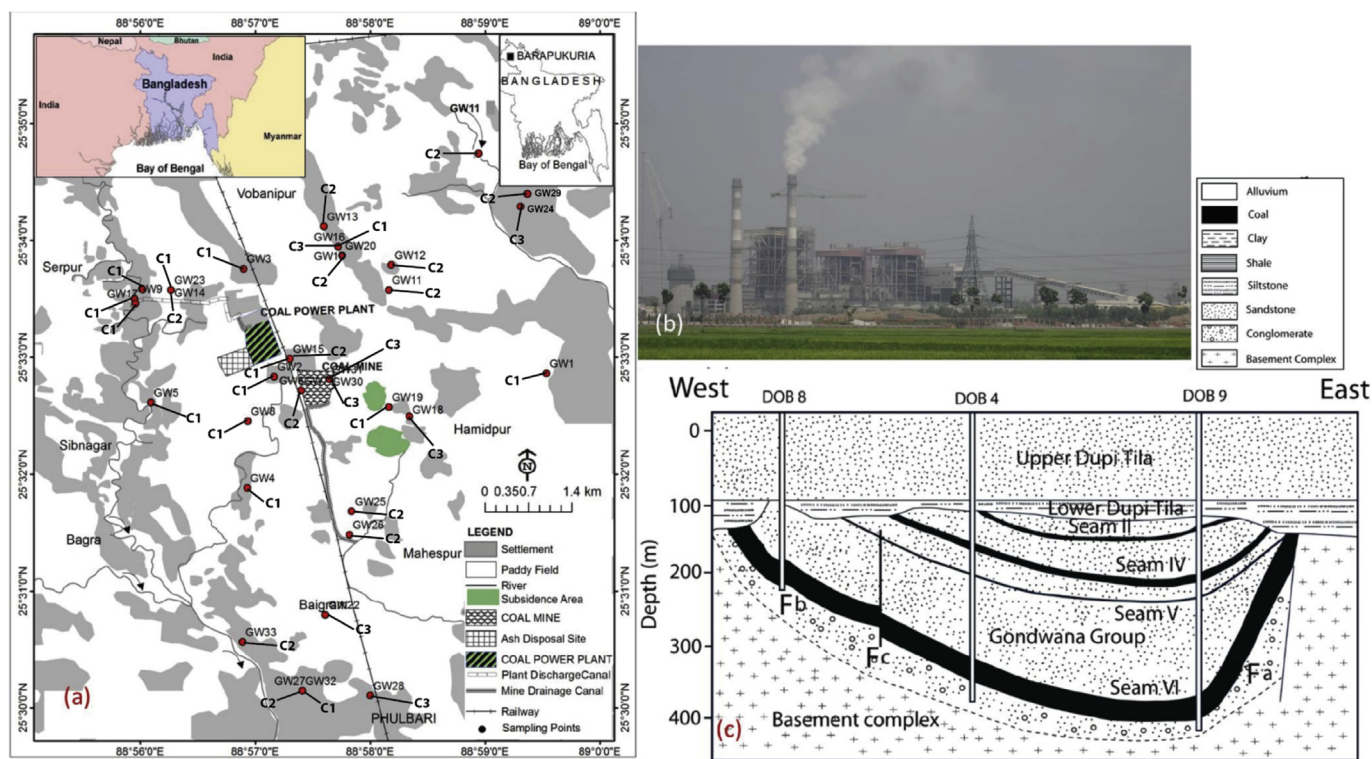


Fig. 1. Study area and location of groundwater sampling sites in the Barapukuria coal basin, b) Barapukuria coal-based power plant (BCPP), c) schematic view of Barapukuria aquifer (groundwater reservoir) with coal seams indicating black color. (For interpretation of the references to color in this figure legend, the reader is referred to the Web version of this article.)

and overexploitation of groundwater are high in the dry season and groundwater recharge is relatively low because of little rainfall occurs in that time. At the same time, groundwater level has substantially reduced in each year in the dry season. However, due to heavy rainfall from June to September during the monsoon season, groundwater recharge and groundwater table are uplifted in this coal basin. For this reason, we have chosen the sampling time from March to May during the dry season. Information on the sampling locations and dates of sampling is summarized in [Supplementary Table S1](#). During sample collection period, physicochemical parameters (pH, and EC) were directly measured with a Multiparameter meter (Model: *senionTM156*, HACH, USA). Total dissolve solids (TDS) were measured manually or gravimetrically and total hardness (TH) was determined using titrimetric method. All samples were filtered through a 0.45- μm filter, stored in a 500 mL high density polyethylene (HDPE) bottles, acidified with 1 mL conc. HNO_3 to control the $\text{pH} < 2$ and then stored at low temperature $\sim 4^\circ\text{C}$ ([Ahmed et al., 2019](#)) to avoid any evaporation before the further analysis. A total of 10 trace elements (Ni, Cd, Cr, Mn, Zn, As, Cd, Pb, Fe, and Co) were determined; among them, As concentration was below the detection limit. The Pb, Cd, Cr, and Ni concentrations were measured using the Atomic Absorption Spectrometer (AAS, A-7000, Shimadzu, Japan) at INARS, Bangladesh Council of Scientific and Industrial Research (BCSIR), Dhaka, Bangladesh. The concentration of Co, Cu, Zn, Fe, and Mn in the samples were measured with Flame Atomic Absorption Spectrometer (Model: AA240FS, Varian, Australia) in air/acetylene flame. The AAS instrument uses specific hollow cathode lamp for each metal determination under the conditions as shown in [Supplementary Table S2](#). The standard limits of detection (LODs) for trace metals Co, Ni, Cu, Zn, Fe, Mn, Pb, Cd, and Cr were 0.0198, 0.0022, 0.0062, 0.0075, 0.0677, 0.0031, 0.0012, 0.0003 and 0.0004 mgL^{-1} , respectively. In this research, the certified reference materials (SRM-1640 and SRM-1643 of National Institute of Scientific and Technology, USA) were employed to verify the analytical results and to ensure the data quality. Precision of the analytical method was further monitored by measuring the replicate samples selected randomly (RSD $< 5\%$). Estimated percentages of recoveries were within 90–100%, with $\pm 2\%$ standard deviation.

2.3. Health risk appraisal

Traditional health risk appraisal methods and mathematical models can differ by country and organization, but all used similar principle ([Zhang et al., 2016](#)). Health risk appraisal methods were introduced by [US EPA \(2004\)](#) to determine the intensity of TMs exposure and their tendency according to the toxicity and the response on human health. We employed the health risk appraisal methods proposed by the US EPA. Oral intake and dermal contact are generally regarded to be the major exposure pathways ([Zhang et al., 2016](#); [Ahmed et al., 2019](#)). Thus, chronic daily intake (CDI) from ingestion (CDI_{oral}) and dermal absorption ($\text{CDI}_{\text{dermal}}$) was computed according to the amended Eqs (1) and (2) recommended by the US EPA ([US EPA, 2004](#); [He et al., 2019](#); [Islam et al., 2019](#); [Wu et al., 2009](#)):

$$\text{CDI}_{\text{oral}} = \frac{(\text{CW} \times \text{IR} \times \text{EF} \times \text{ED})}{(\text{BW} \times \text{AT})} \quad (1)$$

$$\text{CDI}_{\text{dermal}} = \frac{(\text{CW} \times \text{SA} \times \text{EF} \times \text{ED} \times \text{CF} \times \text{ET} \times \text{K}_p \times 10^{-3})}{(\text{BW} \times \text{AT})} \quad (2)$$

where, CDI_{oral} and $\text{CDI}_{\text{dermal}}$ indicate the chronic daily intake dose via oral ingestion and dermal adsorption ($\mu\text{gkg}^{-1}\text{day}^{-1}$),

respectively; CW is the mean concentration of the TMs in groundwater (μgL^{-1}); IR is the daily ingestion rate (Lday^{-1}); EF is the exposure frequency (day/year); ED is the exposure duration (year); BW is the average body weight (kg); AT is the average time of exposure (days); SA is the exposed skin area (cm^2); ET is the exposure time (h/day); and K_p is the dermal permeability coefficient in water (cm/h). All the listed parameters were referenced from [Wu et al. \(2009\)](#), [Karim \(2011\)](#) and the [US EPA \(2004\)](#). The parameters are tabulated in [Supplementary Table S3](#), and the K_p values are APPEARED in [Supplementary Table S4](#).

In the current research, both the non-carcinogenic risk (NCR) and carcinogenic risk (CR) related to oral intake of TMs were computed and appraised. The NCR was calculated using the hazard quotient (HQ) ([US EPA, 2004](#)). The hazard index (HI) is the summation of HQs, which present the probable NCR caused by all TMs. The HQ and HI can be computed by the Eqs. (3)–(6) as follows:

$$\text{HQ} = \frac{\text{CDI}}{\text{NCRfD}} \quad (3)$$

$$\text{NCRf}_{\text{Dermal}} = \text{NCRfD} \times \text{ABS}_g \quad (4)$$

$$\text{HI} = \sum (\text{HQ}_{\text{oral}} + \text{HQ}_{\text{dermal}}) \quad (5)$$

$$\text{HI} = \text{HQ}_1 + \text{HQ}_2 + \dots + \text{HQ}_n \quad (6)$$

where, NCRfD is the non-carcinogenic reference dose for a particular ELEMNT. The $\text{NCRfD}_{\text{oral}}$ and $\text{NCRfD}_{\text{dermal}}$ values are shown in [Supplementary Table S4](#). The $\text{HQ} < 1$ explains the non-existence of deleterious effect on the population, while the $\text{HQ} > 1$ implies a possibility of detrimental effects ([US EPA, 2004](#)).

The carcinogenic risk (CR) is the probability of exposure to a metal causing in cancer over a lifetime period. The CR was computed with the following Eq. (7):

$$\text{CR} = \text{CDI} \times \text{CSF} \quad (7)$$

where, CSF is the oral cancer slope factor ($\mu\text{g/kg/day}$) $^{-1}$. In this study, we only computed the CR for Cr and Cd, because both metals were the carcinogenic elements among the examined TMS. The CSF values of Cr and Cd were 41,000 and 380 $\mu\text{g/kg/day}$ for oral intake exposure, respectively ([Yang et al., 2012](#)). The acceptable ranges (1×10^{-6} to 1×10^{-4}) of the CR values were adopted by the [US EPA \(2004\)](#).

The uncertainty can remain in the health risk appraisal. The findings of conventional health risk model were compared with the potential health risk model to evaluate how much impact of input parameter uncertainty. Thus, Monte-Carlo simulation with Crystal Ball software (version 11.1.2.3; Oracle Inc., USA) were applied for the uncertainty and sensitivity study the sensitivity analysis included 1000 trails. The distribution patterns for the analyzed metal concentrations were measured before the simulation to get the parameters for the consequent simulations.

2.4. Statistical analyses

In earlier studies, inverse distance weighting (IDW) has been recognized as an advanced interpolation method that has high accuracy and low bias in comparison with other interpolation techniques ([Islam et al., 2017b](#); [Habib et al., 2018](#); [Ahmed et al., 2019](#)). Thus, to show spatial distribution of TMs, the IDW interpolation technique was applied in the present study. All the spatial maps in the following were made using ArcGIS (version 10.3) software (Environmental Systems Research Institute, USA). SPSS

(Version 22.0) software was used to normalize the raw data and transform data table (Q_{mode} and R_{mode}) for multivariate statistical approaches. The correlation matrixes, principle component analysis (PCA) and hierarchical cluster analysis (HCA) were also performed by SPSS software. The Kolmogorov-Smirnov (K-S) test was used to verify the frequency distribution and homogeneity of the dataset at a significant level of $p < 0.05$. One-way ANOVA test was performed to compare the means of different combinations and parameters at a significance level of 0.05.

3. Results and discussion

3.1. General characteristics of groundwater samples

The common characteristics of the samples from the studied BCB are outlined in Table 1. The concentration of As was below the detection limit, thus, As was excluded from further analysis. In general, the pH values of the samples varied from 5.21 to 8.31, with an average value of 6.44 ± 0.73 , indicating a range of slightly acidic to slightly alkaline characteristics. The total hardness (TH) showed a large variation (range: 12–520 mg L^{-1} with variance 18,367.88). EC concentration ranging from 49.7 to 506 μScm^{-1} was lower than the Bangladesh standard of 2250 μScm^{-1} (DoE, 1997). TDS concentration ranging from 34.8 to 354 mgL^{-1} was much lower than the Bangladesh water quality standard of 1000 mgL^{-1} (DoE, 1997). Based on the mean concentrations of TMs, the trace metals can be divided into two groups: (1) metals of low abundance ($1\text{--}100 \mu\text{g L}^{-1}$) including Cr, Cd and Pb; and (2) metals of high abundance ($>100 \mu\text{g L}^{-1}$) such as Mn, Fe, Zn, Cu, Ni, and Co. The mean concentrations of Fe, Ni, Mn, Pb, Co and Cd were all above the permissible limits of drinking water quality standards set by DoE (1997), BIS (2012) and WHO (2011), except for the average concentrations of Cu, Zn and Cr. Results showed that trace metals like Ni ($20\text{--}800 \mu\text{g L}^{-1}$), Fe ($20\text{--}12400 \mu\text{g L}^{-1}$), Mn ($24\text{--}13100 \mu\text{g L}^{-1}$), Pb ($5\text{--}500 \mu\text{g L}^{-1}$), Cd ($1\text{--}90.6 \mu\text{g L}^{-1}$) and Cr ($1.11\text{--}95.9 \mu\text{g L}^{-1}$) were above permissible limit, except for the concentrations of Co, Zn and Cu. High concentrations of Ni were noticed in the majority of the samples ($n = 19$) while a few samples ($n = 8$) contained the elevated concentration of Pb as compared to water quality standard

(WHO, 2011). However, elevated level of Cd was also observed in the samples ($n = 6$), while an undesirable concentration of Cr was found in only few samples ($n = 2$) in comparison with international standard. The mean TMs concentrations in groundwater in the BCB were higher than the Bangladesh and International standards except for Cu, Zn and Cr (Table 1). Thus, results suggested that abundances of these TMs in the groundwater may be originated from coal mining activities in the studied coal basin.

The statistically differences ($p < 0.05$) had been observed for the studied TMs in groundwater samples of different sampling sites having various distance and directions from the vicinity of the BCB. This was confirmed by using the one-way ANOVA test (between groups and within groups) statistical analysis which indicated that no diverse differences found to the total variance of Co ($F = 1.68$, $p = 0.29$); Cu ($F = 0.62$, $p = 0.81$); Zn ($F = 2.54$, $p = 0.15$); Mn ($F = 0.17$, $p = 0.99$); Pb ($F = 0.25$, $p = 0.25$); Ni ($F = 23.23$, $p = 0.00$); Fe ($F = 37.61$, $p = 0.00$); Cr ($F = 37.91$, $p = 0.00$) and Cd ($F = 0.16$, $p = 0.99$) with distance-direction variations. It also showed that the analyzed TMs were statistically different, indicating that insignificant influence of the BCPP and diverse distribution of TMs concentrations along the sampling sites.

The variances of Cd and Cr were relatively low, which signified that their spatial distributions were comparatively homogeneous while variances of Fe, Mn, Ni, Co, Zn and Pb were elevated, demonstrating that they were spatially inhomogeneous and might have been influenced by man-made activities. The skewness value is an excellent indicator of concentration distributions (Qiu et al., 2018). The Co and Zn had the skewness values less than one, whereas other TMs had skewness values more than one, which implies that the groundwater samples were mostly right-biased relative to the normal distribution (Table 1). Likewise, in case of kurtosis, these TMs concentrations were found to be leptokurtic where their values more than 3, while the Co and Zn concentration were observed to be platykurtic (Islam et al., 2017b).

According to the obtained results, the mean concentrations of TMs followed a descending trend of $\text{Fe} > \text{Mn} > \text{Co} > \text{Zn} > \text{Co} > \text{Ni} > \text{Pb} > \text{Cr} > \text{Cd}$. The descending trends of TMs abundance in the BCB are possibly similar to those of Bhuiyan et al. (2010) where the TMs are in the order of

Table 1
Descriptive statistics of physical parameters and trace metals of the groundwater samples with guideline values in the Barapukuria coal basin, Bangladesh.

Parameters	Descriptive Statistics							Standards			% of samples exceed Bangladesh standard
	Minimum	Maximum	Mean	Std. Deviation	Variance	Skewness	Kurtosis	DoE (1997)	BIS (2012) Acceptable Limit	WHO (2011) Permissible Limit	
pH	5.21	8.3	6.44	0.73	0.53	0.29	0.39	6.5–8.5	6.5–8.5	No relaxation	
EC ($\mu\text{S/cm}$)	49.7	506	203.07	123.61	15,279.73	1.40	1.07				
TDS (mg/l)	34.8	354	108.04	64.51	4161.97	2.00	5.43	1000	500	2000	
Total Hardness (mg/L)	12	520	126.57	135.53	18,367.88	1.57	1.55				
Co ($\mu\text{g/L}$)	3	960	392.91	298.62	89,171.21	0.45	-1.31				
Ni ($\mu\text{g/L}$)	20	800	135.65	134.19	18,005.97	3.99	19.52	100	20	No relaxation	70
Cu ($\mu\text{g/L}$)	10	900	185.68	248.49	61,748.80	2.21	3.83	1000	50	1500	2000
Zn ($\mu\text{g/L}$)	100	730	339.09	173.64	30,152.27	0.71	-0.32	5000	5000	15,000	
Fe ($\mu\text{g/L}$)	20	12,400	1579.09	2368.62	5,610,371.02	3.27	13.50	300	300	No relaxation	48% (16)
Mn ($\mu\text{g/L}$)	24	13,100	1182.61	2465.23	6,077,369.37	3.87	17.51	100	100	300	400
Pb ($\mu\text{g/L}$)	5	500	68.02	114.97	13,218.51	2.66	7.11	50	10	No relaxation	10
Cd ($\mu\text{g/L}$)	1	90.6	8.02	16.48	271.62	4.41	21.01	5	3	No relaxation	3
Cr ($\mu\text{g/L}$)	1.11	95.9	12.00	17.77	315.68	3.97	16.89	50	50	No relaxation	50

Fe > Zn > Mn > Pb, which followed by Halim et al. (2013) in the sequence of Fe > Mn > Zn > Ni > Cu > Pb > Cr but are different to that of Singh et al. (2018) in the following order of As > Pb > Zn > Mn > Cr > Cu > Ni > Cd.

Table 2 shows a comparison of selected TMs in groundwater in the BCB from this study with those of other coal basins in the world. Compared with the previous study in the coal basin of Bangladesh, the average concentrations of Fe, Mn, Zn, Pb, Ni, Co, Cr, Cu, and Cr in the basins were significantly greater than that of northwest coal basin, Bangladesh (Bhuiyan et al., 2010; Halim et al., 2013). Besides, all TMs concentrations in the BCB were noticeably larger than those in the Karanpura coal basin, India (Neogi et al., 2018); Mugla coal basin, Turkey (Baba et al., 2003); Korba coal basin, India (Singh et al., 2017); Linhuan coal basin, China (Qiu et al., 2018); Bokaro coal basin, India (Tiwari et al., 2017); Thrace coal basin, Turkey (Erarslan et al., 2014); the Dingji coal basin, China (Zhang et al., 2016). However, the average Cr concentration in the coal basin was lower than those in the Raniganj coal basin, India (Singh et al., 2010); the Korba coal basin, India (Singh et al., 2017) and the Tshikondeni coal basin, South Africa (Nephalama and Muzerengi, 2016). Similarly, the mean Fe and Pb concentrations were lower than that of the earlier study of this coal basin (Bhuiyan et al., 2010). Additionally, the mean Mn concentration was significantly lower than those in the Jharia coal basin, India (Prasad and Kumari, 2008). The average Cd content was also significantly lower than that of Tshikondeni coal basin, South Africa (Nephalama and Muzerengi, 2016). Finally, these obtained results revealed that the contamination level of TMs in the studied coal basin exhibited comparatively higher than in other coal basins worldwide.

3.2. Spatial distribution of TMs

The spatial distribution of TMs concentrations in the water samples from the BCB obtained by the inverse distance weighting method is outlined in Fig. 2. The spatial distribution maps showed a high degree of variation of the TMs concentrations in groundwater. In general, distribution and transport of TMs in groundwater depend on the particular metal occurrence and the characteristics of the intrinsic environment. Fig. 2 exhibit that the distributions of Co, Zn, Mn and Pb indicate similar spatial patterns, although their mass concentrations are different. This indicates that these metals likely originate from a similar source. In contrast, the concentrations of Fe, Cd and Cu showed the irregular diverse spatial patterns compared to the other TMs and they did not show any association among them (Fig. 2). Further, a similar pattern between Ni and Cr was observed but these differ from Mn, Zn, Co and Pb. The higher concentrations of Fe, Mn, Ni, Pb, and Cd were found near coal mine area which likely influenced by the anthropogenic attribution. Mn

could have leached out during transport of flying coal dust and ash residues in the basin, whereas Mn oxides from coal mine are predominant substrates of Pb, thus, this can explain their similar spatial variations. Hot spots for Fe, Mn, Ni, and Pb are located in the BCPP. Elevated concentrations of these TMs in the basin may be attributed to the direct consequences of the BCPP operation and in areas within a 2 km radius from the point source BCPP likely owing to the wet and dry deposition of the flying coal-dust and the large amount of fly ash around BCPP. Halim et al. (2013) attributed the enhanced of Fe and Mn due to the discharge point of the BCPP and in the BCB.

Bhuiyan et al. (2010) reported that the elements like Mn, Fe, Co, Ni, Cu and Pb are comparatively higher in groundwater of the BCB area than the Bangladesh and international standards which is mainly related to anthropogenic sources. Authors also reported that about 65% of the area is greatly contaminated with elevated concentration of health sensitive TMs. The groundwater contaminants e.g., Cd, Pb and Cr are regarded as a great threat for local inhabitants and may pose acute and chronic diseases like kidney problem, dysfunctions of liver and cancer (Finkelman et al., 2018). In contrast, the high concentration of Fe (n = 19), and Mn (n = 26) can be a consequence of the geogenic sources. In the study basin, there reductive dissolution of Mn/Fe oxyhydroxides in addition to organic matter might have been a possible source of these metals (Dai et al., 2012). Similarly, a study carried out by Halim et al. (2013) showed that the Fe and Mn in the basin originated from natural source which may have been released from mobilization of parent rock with organic matters. Fe and Mn are regarded as secondary contaminants in terms of health risk because these elements do not cause a high health risk for humans (Dai et al., 2012; Sengupta and Agrahari, 2017; Singh et al., 2018). High concentrations of both TMs in drinking water provide a distasteful metallic taste, and discolor food. Nevertheless, oral ingestion of high Ni (n = 23), Pb (n = 8) and Cd (n = 5) containing drinking water can severely affect human health and could pose different diseases including chronic bronchitis, reduced lung function, and skin cancer (Silva et al., 2013). However, various sources of contamination may affect the distribution patterns of TMs, hence to understand the sources and pathway of contamination, an in-depth statistical study is necessary.

3.3. Sources of TMs

Potential sources of the physicochemical entities and TMs were recognized by combining correlation matrix studies and principal component analysis (PCA). The Pearson correlation analysis of physicochemical properties and TMs in the groundwater of the BCBs is shown in Table 3. Major physicochemical parameters in the

Table 2
Comparison of trace metals concentrations (μgL^{-1}) in groundwater samples from the investigated coal basin in Bangladesh and other coal basin worldwide.

Coal basin (Location)	Co	Ni	Cu	Zn	Fe	Mn	Pb	Cd	Cr	Reference
Barapukuria coal basin (Bangladesh)	392.91	135.65	185.68	339.09	1579.09	1182.61	68.02	8.02	12	This study
Barapukuria coal basin (Bangladesh)	NA	NA	NA	290	5400	26	70	NA	NA	Bhuiyan et al. (2010)
Karanpura coal basin (India)	BDL	15.49	2.36	46.8	1406.5	1161.2	NA	NA	2.04	Neogi et al. (2018)
Korba coal basin (India)	NA	NA	24.08	180.04	150	110	16	2.17	50	Singh et al. (2017)
Bokaro coal basin (India)	NA	21	41	33	880	53	NA	NA	2.4	Tiwari et al. (2017)
Raniganj coal basin (India)	0.95	45.6	18.7	60.1	329	39.4	22.7	0.5	44.6	Singh et al. (2010)
Jharia coal basin (India)	NA	NA	7.5	316	115.6	1706.2	NA	NA	3.9	Prasad and Kumari (2008)
Thrace coal basin (Turkey)	1.28	19.1	3.36	15.37	1350.12	299.29	0.25	0.02	19.75	Erarslan et al. (2014)
Mugla coal basin (Turkey)	BDL	BDL	25	82.7	323.4	433.5	60.4	8.5	26	Baba et al. (2003)
Linhuan coal basin (China)	NA	0.14	0.06	0.42	NA	104.63	0.01	0.03	0.08	Qiu et al. (2018)
Dingji coal basin (China)	NA	2.41	2.92	260.13	0.12	66.57	0.81	0.17	7.91	Zhang et al. (2016)
Tshikondeni coal basin (South Africa)	NA	NA	70	80	90	100	120	30	380	Nephalama and Muzerengi (2016)

BDL = Below Detection Limit. NA = Not Applicable.

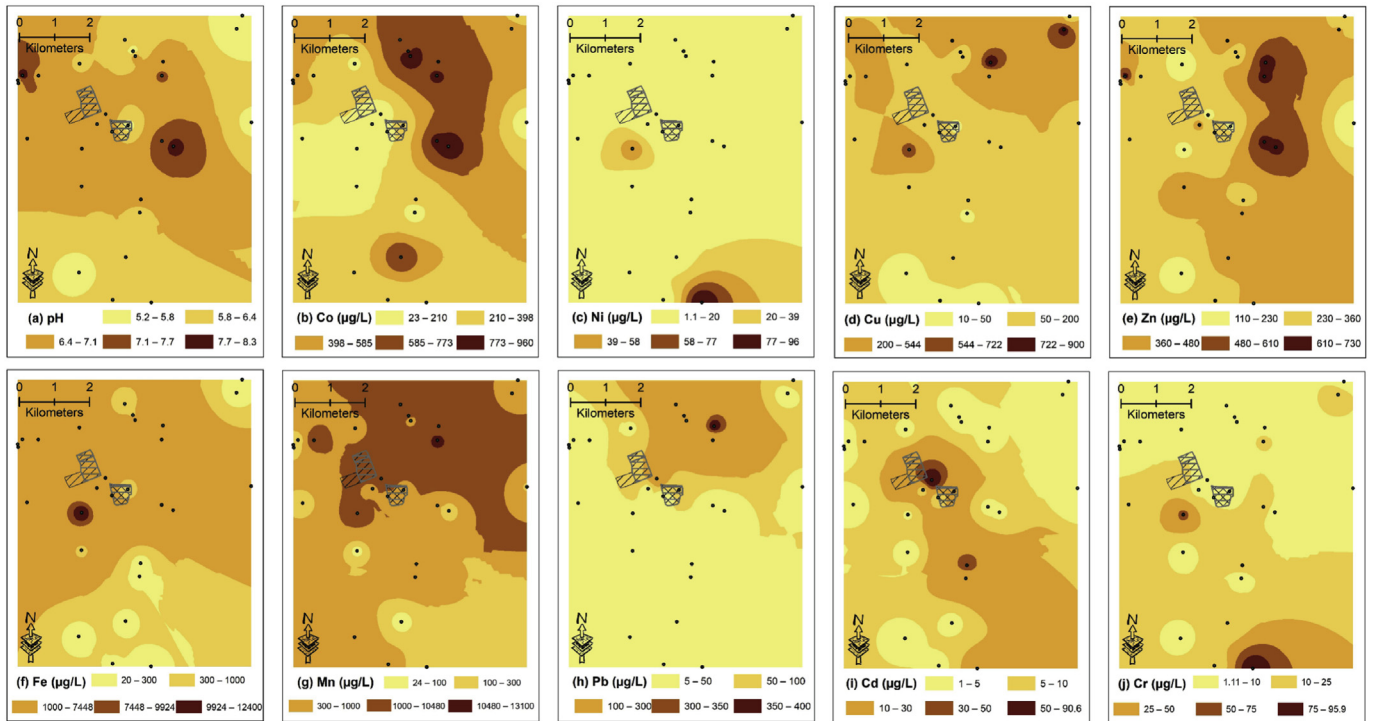


Fig. 2. Spatial distribution maps of pH, Co, Ni, Mn, Pb, Cu, Zn, Fe, Cd and Cr in groundwater of Barapukuria coal basin, Bangladesh.

basin like pH, EC and TH, had significant positive correlations with the TMs ($r_{\text{pH-Zn}} = 0.54$, $r_{\text{EC-TDS}} = 0.88$, $r_{\text{EC-Co}} = 0.52$, $r_{\text{TH-Pb}} = 0.67$, $r_{\text{TH-Fe}} = 0.46$, and $r_{\text{TH-Mn}} = 0.50$, $p < 0.01$). Furthermore, a significant positive correlation was observed in the metal pairs such as Co and Zn ($r = 0.61$, $p < 0.01$); Mn and Pb ($r = 0.57$, $p < 0.01$). Such significant positive relationship invokes the same pathways (geogenic or anthropogenic) and leaching and migration of TMs (Haloi and Sarma, 2012). By contrast, insignificant relationship was found in other elements which indicated that the pathways of these elements were independent from each other indicating likely different sources (Islam et al., 2017b). To explore the elemental associations and their pathways, PCA was carried out for the physicochemical parameters and TMs in the samples from the BCB. In addition, Kaiser-Meyer-Olkin (KMO) test and the Bartlett's Test of Sphericity have used to check the acceptability of the PCA results. The KMO value was 0.52 and Bartlett's Test of Sphericity was assumed to be significant ($p < 0.05$). This indicated that parameters used in the present study are appropriate for PCA. However, the

scree plot is used to identify the number of PCs to be retained to recognize the physicochemical variables and TMs (Fig. 3a). The loading map of the three most influential factors from the PCA is presented in Fig. 4b. Based on the scree plot results, eight PCs explained 91.78% of the total variance in the rotated R-mode data matrix.

Mn, Pb and TH had high positive loadings in PC1, which accounted for 16.93% of the variance (Supplementary Table S5) which was also confirmed by their shared cluster 3 in HCA where Mn showed most similarity with Pb and TH (Fig. S1a). PC1 was mainly distributed in GW10-13 sampling sites in the coal basin (Supplementary Table S4). Mn is a siderophile element, which may be derived from parent rock weathering and pedogenic processes (Islam et al., 2017b). This process was confirmed as the major pathway of Mn based on the high positive correlation between Mn and Pb ($r = 0.57$, $p < 0.01$), suggesting similar natural sources controlled by anaerobic bacteria for releasing Mn and Pb into the groundwater (Bodrud-Doza et al., 2016). The possible source of Pb

Table 3
Pearson correlation matrix of trace metals in groundwater in the Barapukuria coal basin.

	pH	EC	TDS	TH	Co	Ni	Cu	Zn	Fe	Mn	Pb	Cd	Cr
pH	1												
EC	-0.09	1											
TDS	-0.14	.88 ^a	1										
TH	0.05	.35*	0.07	1									
Co	0.21	.52 ^a	.36*	0.17	1								
Ni	-0.24	-0.01	0.04	-0.01	0.11	1							
Cu	0.05	-0.12	-0.21	.35*	0.23	-0.06	1						
Zn	0.54 ^a	0.21	0.15	0.13	.61 ^a	0.02	0.25	1					
Fe	0.33*	0.03	-0.06	.46 ^a	-0.02	-0.07	0.29	0.08	1				
Mn	0.17	0.23	0.14	.50 ^a	0.18	-0.05	0.13	0.27	0.24	1			
Pb	-0.13	0.29	0.05	.67 ^a	0.22	0.11	0.25	0.17	0.01	.57 ^a	1		
Cd	0.12	-0.07	-0.04	-0.15	-0.26	-0.08	-0.14	-0.17	-0.13	0.17	0.14	1	
Cr	0.05	-0.09	-0.02	0.08	-0.17	-0.06	0.08	0.05	0.32*	-0.04	-0.12	0.07	1

^a Correlation is significant at the 0.01 level (2-tailed). * Correlation is significant at the 0.05 level (2-tailed).

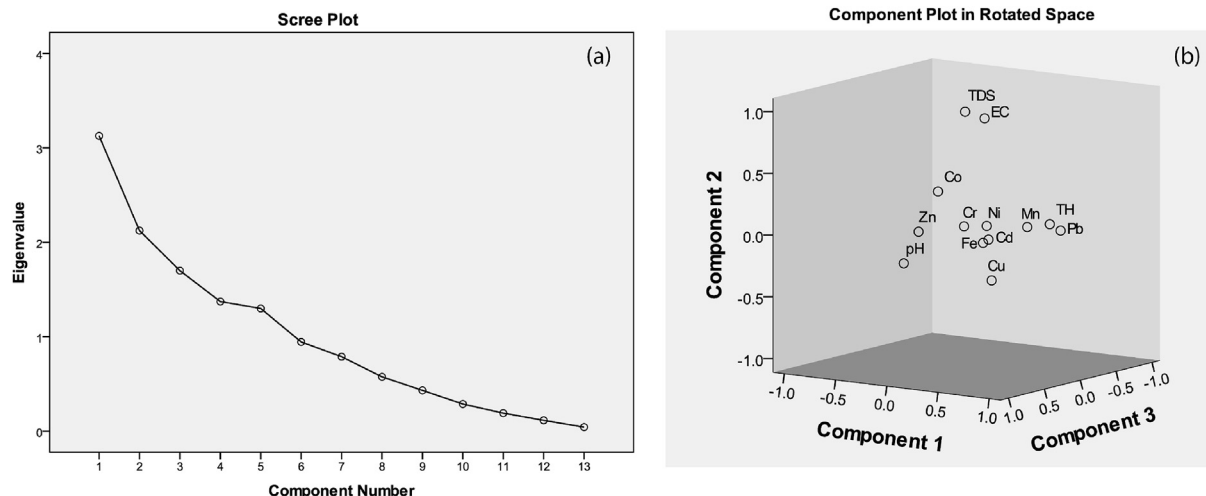


Fig. 3. Principal component analysis by (a) scree plot (eigen values), and (b) component plot in rotated space.

is mainly ascribed to the man-made sources through agrochemical and coal mining wastes (Bhuiyan et al., 2010). The EC and TDS exhibited high loading in PC2, which explained the 16.45% of the variance and was also confirmed by their supportive cluster 1 (Fig. S1a). PC2 was mostly distributed in GW10, GW16, GW18-19 and GW-31 sample locations. EC and TDS are generally originated from geogenic process like weathering of bed rock materials (feldspar and evaporite) in the groundwater system.

The Co, Zn and pH showed a high positive loading in PC3 and accounted for the 14.50% of the total variance and also coincided with their mutual cluster 2 in the hierarchical dendrogram, where Zn exhibited most similarity with Co (Fig. S1a). PC3 was significantly distributed in GW11-12, GW18-19, and GW21 sampling points. Of these, Co and Zn may derive from anthropogenic sources, such as plant and mine effluents (Halim et al., 2013). These were supported by the significant positive correlation between Co and Zn ($r = 0.61$, $p < 0.01$). The possible causes of high Co concentration in the coal basin may be due to small industries and BCPP together with application of fertilizer and agricultural wastes. Hence, Co was released in groundwater and remained in the ionic state. The prime source of Zn in groundwater may be due to extensive phosphate fertilizer and pesticides used in agricultural field (Islam et al., 2017a).

As such, Fe elucidated high positive loading with a loading of 0.92 in PC4 for GW8, GW11 and GW19 samples, which explained 9.94% of the total variance. Both Fe was distantly grouped in cluster 4 (Fig. S1a). Iron was mainly derived from chemical weathering and/or leaching of mine effluents. Iron was regarded a normalizer metal that primarily may originate from natural hydro-chemical weathering of rock (Ahmed et al., 2019). Under alkaline conditions (pH 5.2-8.3), this absorbed metal was possibly again released into the water (Díaz et al., 2016).

As such, Cd accounted for the highest positive loading in PC5, with a loading value of 0.98 while Cu exhibited high positive loading of 0.93 in PC6 which elucidated 8.95% and 8.62% of the total variance respectively, with distribution in GW8, GW23-24 and GW29 sample sites. The highest concentrations of Cd (GW15 and GW25) were found near to the BCPP which was the major source of effluents from industrial and rural areas. The highest level of Cd at GW15 may be due to contact with parent rock as well as agricultural runoff. The prime contributor of Cd in this basin was the burning of coal, application of fertilizers, domestic sewage disposal and atmospheric aerosol deposition (Singh et al., 2018). Copper

might have anthropogenic contribution such as coal waste material effluent in the sample site GW8, GW12, and GW23-24 (Kumar et al., 2017).

On the other hand, Ni showed high positive loading in PC7 for GW29 sampling location, with a loading of 0.93 while Cr exhibited the highest positive loading of 0.98 in PC8, which explained 8.27% and 8.11% of the total variance respectively. Ni was attributed to background concentration that reflected the influence of anthropogenic activities. Industrial wastes, coal power plants, and discarded batteries are most common pathways of Ni pollution (Singh et al., 2018). Groundwater might have acted as an agent for dispersion of Ni from its source area (Bodrud-Doza et al., 2016). In addition, the high concentration of Cr is attributed to the groundwater due to anthropogenic input. The Cr may have been caused by leaching of coal effluents from nearby coal industry. The higher concentration of Cr was observed in sampling site GW8 and GW28 which is near to coal industry. Yellowish brown color of the groundwater was noticed at this point. Chromium was found in low concentration in the rest of samples except for GW8 and GW28. The mean value of Cr, $3.39 \mu\text{gL}^{-1}$ (Halim et al., 2013) and $44.6 \mu\text{gL}^{-1}$ (Singh et al., 2010) and $19.75 \mu\text{gL}^{-1}$ (Erarslan et al., 2014) were reported in the coal basin of northwest Bangladesh and in the Raniganj coal basin, India, and the Thrace coal basin, Turkey, respectively.

An interesting result in comparing the PCA findings is the similarity in the PCA weight of concentrations as a significant pair between them such as Mn vs Pb, Co vs Zn and EC vs TDS (Fig. 3). The Mn concentration showed high positive loading with Pb in PC1, while Co concentration exhibited high positive loading with Zn in PC3 and EC demonstrated high positive loading with TDS in PC2. It inferred that similar pathway(s) of contaminants were contributing to groundwater contamination. The obtained results indicated that PCA can assist as an important means to identify the major pathways contributing groundwater contamination in the BCB.

3.4. Potential pathways identification of TMs

The R-mode hierarchical cluster analysis (HCA) retained six major clusters for datasets of measured groundwater samples. R-mode HCA was used to understand physicochemical variables and TMs groupings in the datasets (Fig. S1a). Variables belonging to the similar cluster were likely to be originated from similar pathway. HCA grouped the analyzed variables into six clusters: cluster 1

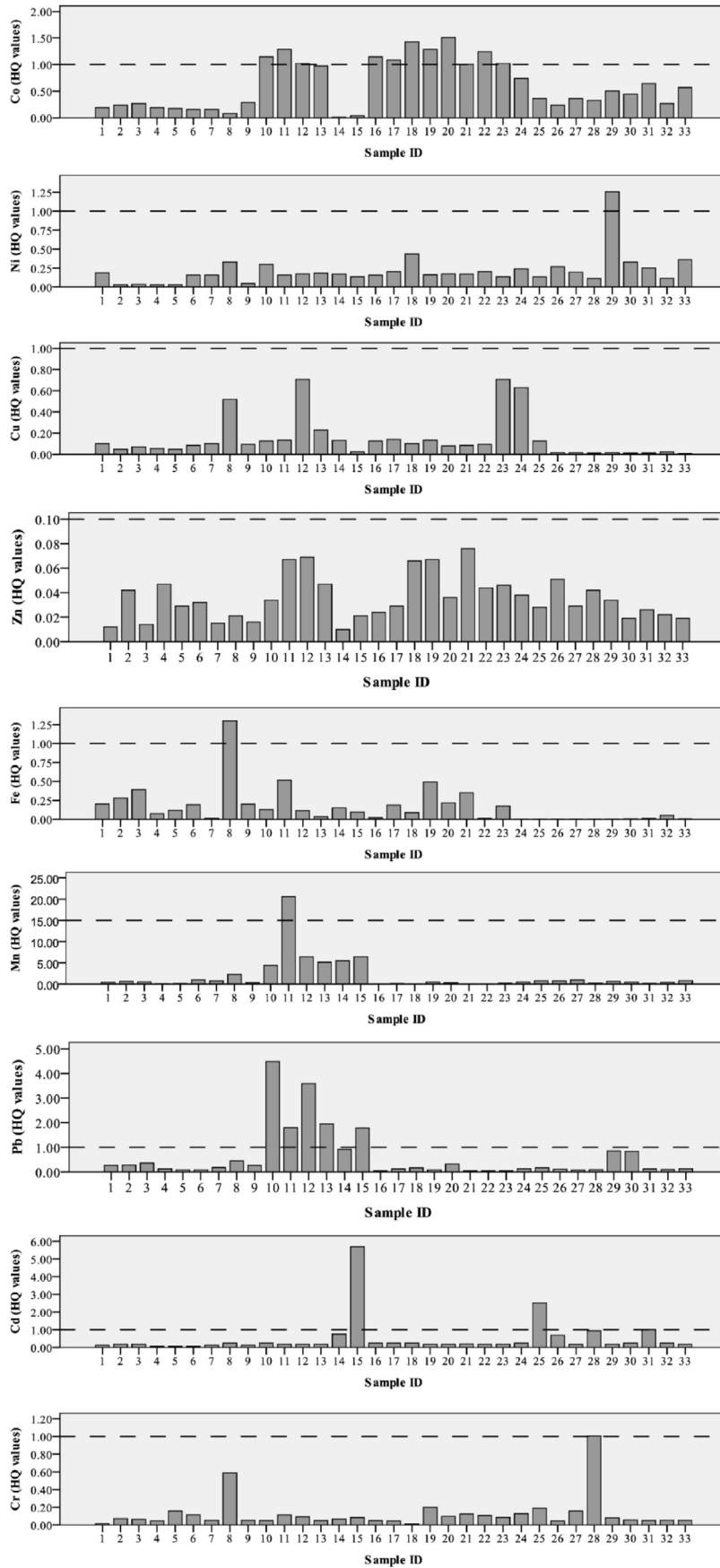


Fig. 4. Non-carcinogenic health risk appraisals for adults via oral ingestion HQ for each metal.

included EC and TDS which loaded positively in PC2; pH, Co and Zn which loaded positively in PC3 grouped into cluster 2; cluster 3 comprises TH, Mn, Pb and Cu as loaded positively in PC1; Fe and Cr as loaded positively in PC4 constitute cluster 4. Clusters 5, and 6 contained Ni (negatively loaded in PC5) and Cd (highly negative loaded in PC5) respectively. Thus, the results of HCA are agreed well with the results of PCA.

Q-mode HCA was applied to identify the spatial similarities and sites grouping among the sample locations (Fig. S1b). Specific group/class revealed analogous characteristics with respect to the analyzed variables in a samples clustering. The HCA of the 33 sampling sites constitutes three clusters. The cluster 1 consists of 14 sampling points including GW32, GW23, GW4, GW20, GW17, GW6, GW5, GW21, GW19, GW2, GW9, GW3, GW8 and GW1; cluster 2 covers 12 sampling points (GW7, GW29, GW10, GW15, GW14, GW11, GW13, GW12, GW26, GW25, GW33 and GW27) and Cluster 3 comprises seven samples such as GW22, GW16, GW18, GW30, GW31, GW28 and GW24. The percentages of cluster 1, 2 and 3 are about 36.36%, 21.21% and 42.42%, respectively with respect to the total sampling points. Clustering of sampling sites (Supplementary Table S5) revealed that the samples from the points GW8, GW10–13, GW15–24, and GW28–31 were more contaminated compared to other sampling sites according to the analyzed pollutants. This cluster 1 site is closed to near BCB and highly groundwater pollution occurred via anthropogenic activities while cluster 2 and cluster 3 sites are mostly comparatively less contamination than cluster 1 due to leaching of coal effluences and agrochemical inputs (Fig. 1). It is therefore not surprising that cluster 2 (GW27 and GW29), and cluster 3 (GW16 and GW24) were grouped together in the same cluster. The outcomes of HCA are compared with the result of sites grouping in the sampling sites, indicating groundwater vulnerability in the coal basin area (Fig. 1).

3.5. Probable health risks assessment

3.5.1. Non-carcinogenic risk appraisal of TMs

There is no prior investigation to appraise the probable human risk in the local residents of the BCB. Based on the traditional health risk model suggested by the US EPA, 2004, the non-carcinogens (NCR) and carcinogens risks (CR) to individual health of the TMs in groundwater from the studied basin were estimated. The computed values of HQ_{oral} , HQ_{dermal} and HI are displayed in Table 4. Overall, in case of NCR, the HI_{oral} and HI_{dermal} values for both age populations exceeded the safe limits (>1) except for HI_{dermal} adults (Table 4), indicating that apparent health risk was observed in groundwater from the BCB. The HQ_{oral} , and HQ_{dermal} for children were larger than those for adults in this BCB, indicating that children are more susceptible and exposed to the effect of health hazards of TMs exposure from groundwater, which is similar to earlier findings elsewhere in Bangladesh (Islam et al., 2017c, 2019; Rahman et al., 2018; Ahmed et al., 2019). Especially, the HQ_{oral} of the TMs values ranged from 1.85 to 3.55×10^{-2} for adults and 2.35 to 4.51×10^{-2} for children. These findings suggested that oral exposure had unpleasant health impacts on health and caused potential NCR. The HQ_{dermal} values of the TMs in adults and children were below 1 (adults: 1.11×10^{-1} to 2.18×10^{-3} , children: 2.02×10^{-1} to 3.87×10^{-3}), demonstrating that the studied TMs showed insignificant health risk via dermal absorption than oral ingestion exposure.

The HQ_{oral} mean values in the coal basin showed in the descending order of $Mn > Co > Pb > Cd > Ni > Fe > Cu > Cr > Zn$, respectively for both age groups while the HQ_{dermal} mean values followed the descending order of $Cd > Mn > Cr > Pb > Fe > Ni > Cu$, respectively. In fact, the average HI values of groundwater pollutants for children are much greater than unity irrespective of oral

and dermal NCR, demonstrating that a detrimental NCR existed in the coal basin. Children had much greater values of NCR than adults such as the HI average of TMs is higher than one in the measured samples, indicating the NCR impact of TM contaminants on children in this basin (Fig. S2). It is evident that Mn, Pb, Cd and Cr play a vital role in causing NCR for both the age population groups. Zinc and Cu concentrations contribute less than those of other TMs. In general, total HI_{oral} of NCR from Mn, Co, Pb, Cd, Ni, Fe, Cu, Cr, and Zn concentrations is 1.1 times greater for children than adults. In the case of HI_{oral} , high undesirable level of health risks for adults and children are presented for all the studied samples, where high chronic risks were observed more than 99% samples while in case of HI_{dermal} , low chronic risk were found more than 27% samples (Supplementary Tables S6 and S7).

The obtained values from HI_{oral} for all TMs are comparatively higher and above the range of safe limits (>1) than that of HI_{dermal} suggesting the high risk for both the age groups. This study also depicted that the ingestion exposure and dermal absorption rate for children are notably very high as compared to adults which may possibly form detrimental effects to large population groups. In addition, groundwater of all sampling sites except for the sites of GW4 and GW5 is highly contaminated and at risk due to detrimental level of TMs exposure to both age groups through ingestion pathway while 20% of sampling sites are highly hazardous because of undesirable level of TMs exposure to both population via dermal absorption.

In this study, indices like Hazard Quotient (HQ) and Hazard Index (HI) were calculated for two population groups based on the US EPA standards for rate of oral ingestion and dermal absorption. The estimated HQ values for each trace element through oral ingestion for adults are shown in Fig. 4. Similarly, the estimated HQ values for each trace element via oral intake for children are displayed in Fig. S2. For oral ingestion, the exceeded HQ values of Co ranged from 1.01 to 1.92 for the GW10–13, and GW16–23 sampling sites. In the case of Ni, the HQ value was observed to be 1.60. The HQ value for Fe was also exceeded the prescribed limit 1 for sample GW8 (1.65). Mn was found to be above the safe limit with values of 5.6, 26.2, 8.2, 6.56, 6.96, and 8.2 in sample sites (GW10–15), respectively. In all samples, the HQ values for Pb also exceeded the threshold level 1 and ranged from 1.16 to 5.71. Cadmium was found to be above the safe limit with a value of 7.25 in sample GW15. In the case of dermal absorption, Mn exceeded the safe limit 1 with values 4.15, 1.30, 1.04, 1.10 and 1.30 in samples GW11–15, respectively. Cadmium was attained found to be above the recommended limit in sample GW15 with HQ value of 4.58. The high values of HQ found in few sites, if used as drinking water, may be enhanced the health risk to population residing around BCB (Ma et al., 2012). The exposed population is assumed to be safe in values $HQ < 1$ while $1 < HQ < 5$ indicates that the exposed population is in a level of concern. In the study area $HQ > 5$ were found for Mn at locations GW11–15. The HQ values were greater than 1 with respect to these TMs for all other sampling sites, thus, the health risks of TMs exposure via drinking water was supposed to be unsafe (Supplementary Tables S8 and S9).

To understand the cumulative risk from oral ingestion pathway, the calculated HI values are shown in Fig. 5a and b for adults and children, respectively. It is impossible to predict accurate health impact in terms of HI. The HI can add the strength of risk contributed to each component of the mixture (Rahman et al., 2018). If the HI exceeded unity, the concern is the same as if a single exposure exceeded its permissible level by the same proportion (US EPA, 1986). The unity value of HI ranged from $1 > HI > 5$, and nearly 85% fall within this limit except the GW11–15 sampling points and $HI > 5$ was found in 15% of the samples suggesting high risk level for oral ingestion. The HI can be used to identify the elements that have

Table 4

Hazard quotient (HQ) and Hazard index (HI) of each investigated trace metals regarding non-carcinogenic and carcinogenic risk in the groundwater samples collected from Barapukuria coal basin.

Trace metals		NCR HQ _{oral}		NCR HQ _{dermal}		NCR HI _{oral+dermal}		CR _{oral}	
		Adults	Children	Adults	Children	Adults	Children	Adults	Children
Cd	Min	6.3×10^{-2}	8.0×10^{-2}	2.34×10^{-1}	5.1×10^{-2}	1.22×10^{-1}	3.5×10^{-2}	1.19×10^{-5}	1.52×10^{-5}
	Max	5.59	7.25	2.39×10^{-1}	4.58	5.76×10^{-1}	3.10	1.08×10^{-3}	1.38×10^{-3}
	Mean	5.04×10^{-1}	6.41×10^{-1}	2.29×10^{-1}	4.06×10^{-1}	3.52×10^{-1}	6.62×10^{-1}	9.57×10^{-5}	1.22×10^{-4}
Cr	Min	1.20×10^{-2}	1.50×10^{-2}	1.17×10^{-1}	1.90×10^{-2}	1.32×10^{-1}	1.39×10^{-1}	1.43×10^{-3}	1.83×10^{-3}
	Max	1.01	1.28	1.19×10^{-1}	1.62	1.79	3.88	1.24×10^{-1}	1.57×10^{-1}
	Mean	1.25×10^{-2}	1.60×10^{-2}	1.11×10^{-1}	2.02×10^{-1}	7.56×10^{-1}	1.34	1.55×10^{-2}	1.97×10^{-2}
Cu	Min	8.0×10^{-3}	1.01×10^{-2}	2.18×10^{-3}	0	1.09×10^{-1}	0	–	–
	Max	7.07×10^{-1}	9.0×10^{-1}	2.22×10^{-3}	1.9×10^{-3}	6.61×10^{-1}	1.9×10^{-2}	–	–
	Mean	1.45×10^{-1}	1.85×10^{-1}	2.18×10^{-3}	3.87×10^{-3}	4.48×10^{-1}	8.37×10^{-3}	–	–
Mn	Min	0	0	2.16×10^{-1}	8.0×10^{-3}	1.09×10^{-1}	5.5×10^{-3}	–	–
	Max	20.59	26.2	2.22×10^{-1}	4.14	2.35×10^{-1}	2.35	–	–
	Mean	1.85	2.35	2.11×10^{-1}	3.74×10^{-1}	2.36×10^{-1}	4.25×10^{-1}	–	–
Fe	Min	2.0×10^{-3}	3.0×10^{-3}	4.97×10^{-3}	0	4.48×10^{-3}	4.0×10^{-3}	–	–
	Max	1.29	1.65	4.87×10^{-3}	7.0×10^{-3}	1.17	2.11	–	–
	Mean	1.65×10^{-1}	2.11×10^{-1}	5.0×10^{-3}	8.84×10^{-3}	2.37×10^{-1}	5.26×10^{-1}	–	–
Ni	Min	3.1×10^{-2}	4.0×10^{-2}	3.68×10^{-3}	1.0×10^{-3}	2.34×10^{-3}	1.0×10^{-3}	–	–
	Max	1.26	1.6	3.76×10^{-3}	3.8×10^{-3}	1.23×10^{-2}	3.80×10^{-2}	–	–
	Mean	2.13×10^{-1}	2.71×10^{-1}	3.66×10^{-3}	6.39×10^{-3}	7.61×10^{-3}	1.41×10^{-1}	–	–
Pb	Min	4.5×10^{-2}	5.7×10^{-2}	2.35×10^{-1}	3.0×10^{-3}	2.62×10^{-2}	2.7×10^{-2}	–	–
	Max	4.48	5.71	2.21×10^{-1}	3.01×10^{-1}	1.31	2.44	–	–
	Mean	6.11×10^{-2}	7.77×10^{-2}	2.31×10^{-2}	4.09×10^{-2}	2.73×10^{-1}	6.03×10^{-1}	–	–
Zn	Min	1.0×10^{-2}	1.3×10^{-2}	–	–	–	–	–	–
	Max	7.6×10^{-2}	9.7×10^{-2}	–	–	–	–	–	–
	Mean	3.55×10^{-2}	4.51×10^{-2}	–	–	–	–	–	–
Co	Min	5.0×10^{-2}	6.0×10^{-3}	–	–	–	–	–	–
	Max	1.51	1.92	–	–	–	–	–	–
	Mean	6.17×10^{-1}	7.85×10^{-1}	–	–	–	–	–	–

highest health risk. Fig. 5 represents that the HI_{oral} of Mn, Co, Pb, Cd and Cr are the most hazardous metals for both age population groups exist in groundwater of this study area.

The HI_{oral} values of NCR for adults are higher than one in northern, northeastern and central BCPP areas including the Vobanipur, Hamidpur and Sherpur areas (Fig. 1). HI_{oral} values for children are significantly elevated in the central, southeastern, northern and northeastern areas of BCB and BCPP areas. According to the spatial distribution of health risk appraisal of HI_{oral} for both age groups, 48.48% of samples had more than 3 HI values (>3) followed by 48.48% of samples which had less than 3 HI values (<3->1), respectively, whereas only 3.03% of samples had less than 1 HI value (Fig. S3). On the contrary, in the spatial distribution of health risk evaluation of HI_{dermal} for both adults and children, 72.72% of samples had less than 1 HI values (<1) and 27.27% of samples had more than 1 HI values (>1) (Fig. S3). In case of HI_{dermal} of NCR values for adults were elevated in only BCPP area, while the HI_{dermal} values for children were higher than one in southern, northern and central parts including BCM and BCPP, Mahespur, and Phulbari areas.

In the current research, the obtained results also demonstrated that the high HI values are an effect of high content of Mn along with Pb, Ni, Cd, Co and Cr in groundwater. These TMs were also greater than the drinking water quality guideline and earlier reported data of groundwater (Bhuiyan et al., 2010; Halim et al., 2013; Islam et al., 2015). This study also confirmed that local residents would experience severe health risks from the ingestion of each metal according to the oral and dermal absorption pathways of individual TMs.

3.5.2. Cancer risk appraisal of TMs

Among the investigated TMs, Cd and Cr are the elements that present the carcinogenic risks (CR); thus, we computed the CR for Cd and Cr in the study. The CR values are outlined in Table 4. The CR results of Cr in the groundwater pathways were higher (adults:

1.55×10^{-2} , children: 1.57×10^{-1}) than those for Cd (adults: 9.57×10^{-5} , children: 1.83×10^{-3}). The CR ingestion values were above the safe limit (1.0×10^{-6}), demonstrating a high risk of carcinogenicity exposure. In addition, all CR ingestions were greater than 1.0×10^{-6} (the standard adopted by the US EPA, 2004) These findings suggest that Cr could cause more risk to exposed populations through drinking water than that of Cd; hence, future research work and management should be focused on Cr contamination rather than Cd contamination. According to the spatial distribution of CR for Cd for both adults and children, 81.81% of samples had the desirable limit (1.0×10^{-5}) followed by 15.15% of samples which had an acceptable limit (1.0×10^{-4}), while 3.03% of samples had an undesirable limit (3.03%), respectively (Supplementary Table S10). Similarly, in case of Cr for both age population groups, 57.57% of samples had undesirable limit (1.0×10^{-3}) followed by 39.39% (1.0×10^{-2}) and 3.03% of samples had an unsafe level (1×10^{-1}).

The high CR_{oral} Cd values for adults were observed in southeastern and central parts of BCM and BCPP (Fig. S4). It was noticed that similar spatial patterns were found in children as well as adult in the basin. It is FOUND that the chronic risk owing to exposure of contaminated groundwater for both age populations followed in the descending orders central > southeastern > northeastern > southwestern parts of the study basin and this pattern is alike for the cancer risk distribution. On the other hand, the high CR_{oral} Cr values for both age groups showed a homogeneous spatial pattern in the BCB (Fig. S4). An interesting finding is that almost all sampling sites demonstrated more sensitivity to human health risk for children than adults. Rahman et al. (2018) pointed out that children showed 4-fold higher HI for NCR and 1.5-fold higher CR than adults. In the present study, the risk level is more severe via oral ingestion exposure than dermal absorption pathway for both age groups, and similar findings were found in the elsewhere coal mining basin in the Dingji and Linhuan coal basin, China (Zhang et al., 2016; Qiu et al.,

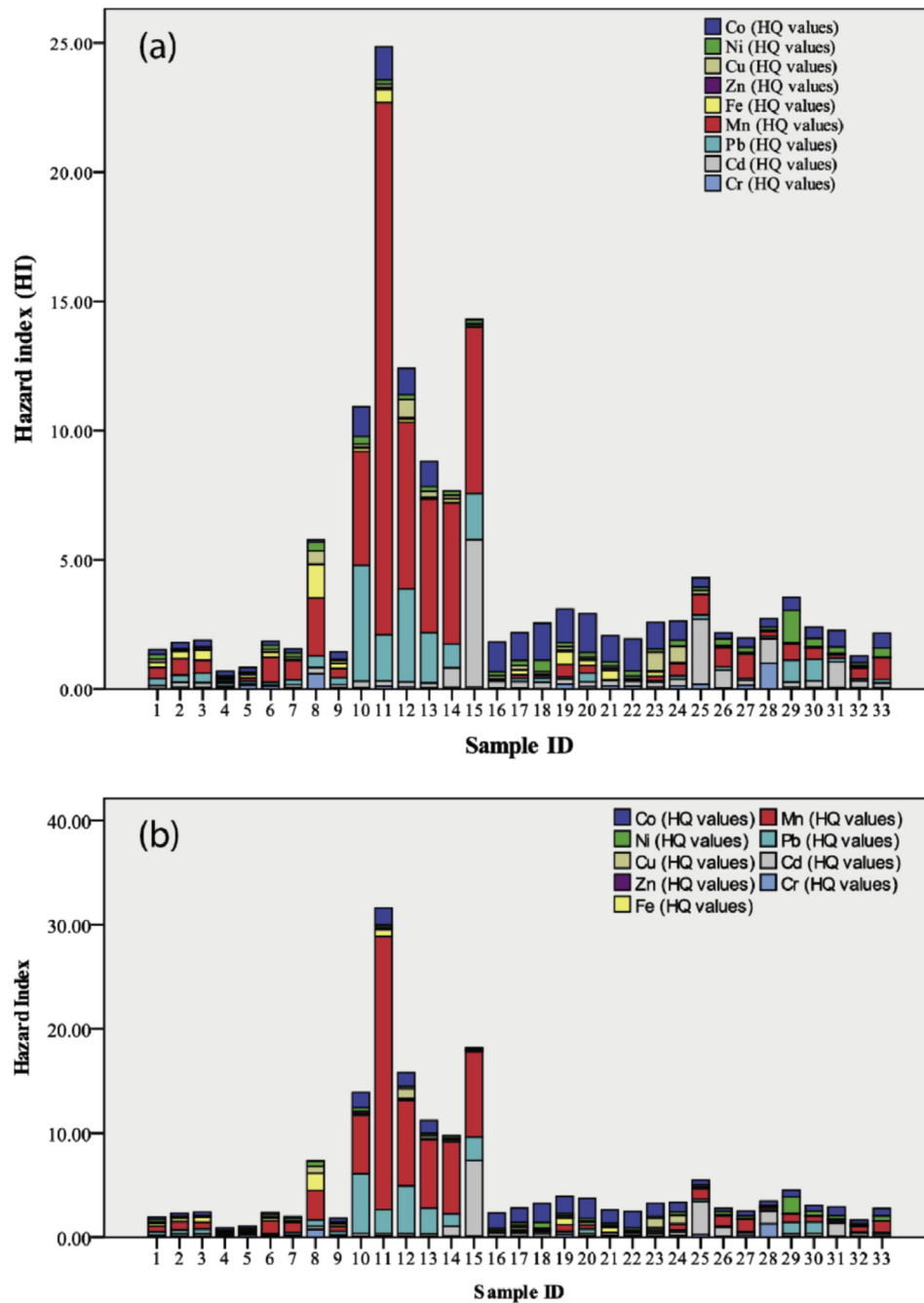


Fig. 5. Non-carcinogenic health risk appraisals for (a) adults and (b) children via oral ingestion HI for trace metals.

2018) and the East Singhbhum coal basin, India (Singh et al., 2018).

Therefore, the carcinogenic risk of Cr and Cd in groundwater resource in the coal basin should draw more attention from drinking water quality management. By calculation, the CR of Cr was accounted for 100% of groundwater samples, while the carcinogenic risk of Cd was accounted for 3.30% (GW15) of the all samples. Therefore, the CR of Cr for both age populations was much elevated than that of Cd, and Cr was the major carcinogenic risk in the BCB.

The Cr content in drinking water is about $1.11\text{--}95.9\ \mu\text{gL}^{-1}$ in the BCB, and is elevated in alkaline water. All the Cr compounds are toxic when the concentrations are high, but the strength of the

toxicity is diverse. Cr exposure will decrease male fertility and the implantation of fetuses and also liver and kidney diseases (Frontasyeva et al., 2001; He et al., 2018). It is noted that Cr^{3+} is usually regarded as non-toxic element and essential for human but it has severe hepatic impacts to human body (Finkelman et al., 2018). In contrast, Cr^{6+} is toxic and easily absorbed in groundwater but, it is generally released by industrial exposures (Frontasyeva et al., 2001). Considering the obtained results of the CR produced by Cr in the BCB, much more focus should be paid to it and proper and efficient counteraction measures should be needed immediately to decrease undesirable impacts on environmental compartments and human health.

3.5.3. Uncertainty and sensitivity analysis in health risk appraisal

Uncertainty is inevitable in health risk appraisal. In the present research, the primary health risk was the Cr of Cr oral intake in both adults and children. Thus, the monte Carlo simulation was used to measure the uncertainty and carry out sensitivity study of the random parameters in the human health risk model. The probabilistic health risk appraisal parameters were applied for a maximum of 1000 trials. The trace metal Cr and the most sensitive group such as children and adults were chosen for appraisal. The parameters include the mean Cr concentration (C of the BCB), IR, EF, ED, AT and BW which were chosen as the random parameters. The uncertainty investigated results are illustrated in [Supplementary Fig. S5](#). In this basin, a gamma distribution pattern had observed in Cr. In the computation of Cr in children, the 5% and 95% probability of iterations varied from 1.13×10^{-2} to 1.38×10^{-1} with a mean value of 6.02×10^{-2} . Similarly, in the case of adults, the 5% and 95% probability of iterations ranged from 9.85×10^{-3} to 1.12×10^{-1} with an average value of 4.89×10^{-2} . These Cr values were exceeded the maximal permissible risk level suggested by the US EPA (1×10^{-6} to 1×10^{-4}). Thus, uncertainty cannot be affected the pollution prevention and control findings in this research.

Sensitivity study was carried out to recognize the contributions of the input parameters to the probable health risk appraisal. The sensitivity study findings of CR in both age population groups exposed to Cr are presented in [Fig. 6](#). The sensitivity of the parameters followed the descending order of $C > EF > ED > IR > BW > AT$ for Adults and in the order of $C > IR > EF > ED > BW > AT$ for children. Higher C, EF, and ED might have elevated positive health risk for adults, and the elevated C, IR and EF would have increased health risk for children. On the other hand, higher AT and BW might have negative impacts on health risk for both age populations. According to these results, C, and AT for both age group populations were the two most influential parameters on the CR of Cr ([Fig. 6](#)). Hence, future water management endeavors should be concentrated on extra controls based on these parameters. [Geng et al. \(2016\)](#) showed that TMs content had the highest positive impact on risk computation of drinking water in two regions of China. [Lu et al. \(2015\)](#) found that As concentration had the maximum positive impact on the CR in Shenzhen, China. [Fallahzadeh et al. \(2017\)](#) reported that heavy metal concentration

had the most influential positive effect on the probable cancer risk in five cities of Iran which is similar to this study.

There are some limitations in the risk appraisal computations in the present study due to the mean values of the TMs were used, and the these used variables were got from the USEPA and WHO, which may be unsuitable to Bangladesh condition. Moreover, the comparatively wide sampling locations of groundwater may result in some uncertainties for spatial-temporal variability of TMs concentration in groundwater. Thus, more detailed research should be performed further in this coal basin with considering the high spatiotemporal variations of TMs in groundwater.

4. Conclusions

Pathways and associated probable health risks of TMs contamination in groundwater from the BCB, Bangladesh were appraised by applying multivariate statistics, traditional health risk model and Monte-Carlo simulation. The following conclusions are drawn from this research:

- The mean concentrations of TMs such as Fe, Mn, Ni, Pb, Cd and Cr) exceeded the acceptable limits for drinking water quality recommended by DoE, Bangladesh, the WHO, and the BIS standards except for the Cu, Zn, and Co at several locations demonstrating an anthropogenic attribution to the groundwater quality. Among the measured TMs, Cd, Cu, Ni, Co, Pb, Cr and Zn derived mostly from anthropogenic activities, while other metals derived from geogenic source i.e. rock-water interaction.
- The results of correlation analysis, and PCA, confirmed by HCA identified mainly man-made inputs including mine and plant waste effluents, agro-chemical, agricultural runoff, and sewage sludge along with natural sources such as weathering of parent rock as major contributing factors of TMs contaminations in groundwater. Further, the findings of Q-mode HCA and PCA implied that the proximal sampling sites near to the BCM and BCPP e.g., GW8, GW10–13, GW15–24, and GW28–33 are highly contaminated by anthropogenic inputs. The elevated concentrations of Fe, Mn, Ni, Pb, Cd and Cr in groundwater were mainly due to quick infiltration and accumulation of heavily toxic mine water in the aquifer.

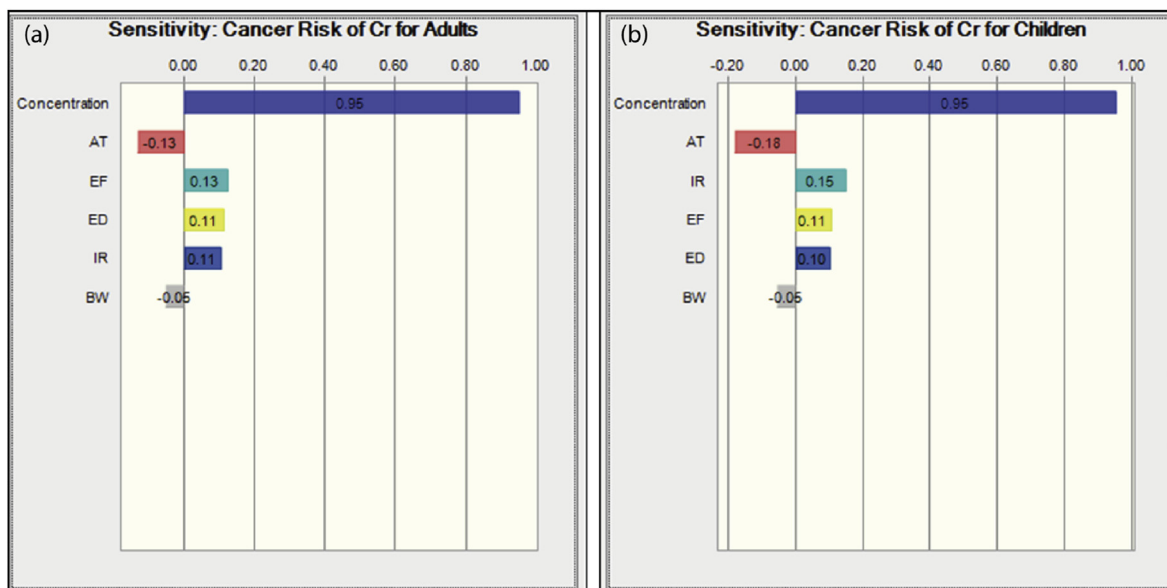


Fig. 6. Sensitivity analysis results to identify the relative contribution of input parameters on the carcinogenic risk caused by Cr for both age group populations.

- Potential health risk appraisal confirmed that these TMs were very high non-carcinogenic risk (NCR) to human health via intake and dermal exposure (i.e., HQ_{oral} , HQ_{dermal} , and $HI > 1$) which may create serious health hazard. Children were more susceptible than adults to the NCR, based on the $HQ_{oral+dermal}$ and $HI_{oral+dermal}$ results for both age population groups. Conversely, the carcinogenic risk (CR) values of Cr were much higher than Cd exposure for adults and children in the BCB, though both surpassed the standard range of 1×10^{-6} to 1×10^{-4} suggested by the US EPA.
- The results of uncertainty assessment for the CR of Cr in both age groups were consistent with the risk appraisal outcomes. Cd, Cr, and Pb are the riskiest metals containing in the coal basin. Overall, the results suggest that the concentration of Cr and the parameter EF for adults and the concentration of Cr and the parameter IR for children require extra attention in terms of health regulation and groundwater management.
- The outcomes of the study around the coal basin may be helpful and utilized for taking proper adaptive steps to alleviate the poorer drinking water quality, in general, and in other similar coal mine basins in the world.

Declaration of competing interest

The authors have no conflict of interest.

Acknowledgements

The authors would like to acknowledge the Thailand's Education Hub for Southern Region of ASEAN Countries (TEH-AC) (Contract No: THE-AC014/2016), grant for financial supports for Doctor of Philosophy Programme in Sustainable Energy Management, Faculty of Environmental Management, Graduate School, Prince of Songkla University (PSU), Thailand. The authors also would like to acknowledge Prof. Dr. J.C. Hower for proofread the whole manuscript. The authority of the Geological Survey of Bangladesh (GSB) and Dept. of Disaster Management, Begum Rokeya University, Rangpur deserves appreciation for its kind support to carry out this research work.

Appendix A. Supplementary data

Supplementary data to this article can be found online at <https://doi.org/10.1016/j.chemosphere.2019.125183>.

References

- Ahmed, N., Bodrud-Doza, M., Islam, A.R.M.T., Hossain, S., Moniruzzaman, M., Deb, N., Bhuiyan, A.B.Q., 2019. Appraising spatial variations of As, Fe, Mn and NO_3 contaminations associated health risks of drinking water from Surma basin, Bangladesh. *Chemosphere* 218, 726–740.
- Baba, A., Kaya, A., Birsoy, Y.K., 2003. The effect of Yatagan thermal power plant (Mugla, Turkey) on the quality of surface and ground waters. *Water Air Soil Pollut.* 149 (1–4), 93–111.
- Bhuiyan, M.A.H., Islam, M.A., Samuel, B., Dampare, S.B., Parvez, L., Suzuki, S., 2010. Evaluation of hazardous metal pollution in irrigation and drinking water systems in the vicinity of a coal mine area of northwestern Bangladesh. *J. Hazard Mater.* 179, 1065–1077.
- BIS, 2012. Drinking Water Specifications 2nd Revision. Bureau of Indian Standards (IS 10500: 2012). New Delhi. <ftp://law.resource.org/jin/bis/S06/IS.10500.2012.pdf>.
- Bodrud-Doza, M., Islam, A.R.M.T., Ahmed, F., Das, S., Saha, N., Rahman, M.S., 2016. Characterization of groundwater quality using water evaluation indices, multivariate statistics and geostatistics in central Bangladesh. *Water Sci* 30, 19–40.
- Dai, S., Ren, D., Chou, C.L., Finkelman, R.B., Seredin, V.V., Zhou, Y., 2012. Geochemistry of trace elements in Chinese coals: a review of abundances, genetic types, impacts on human health, and industrial utilization. *Int. J. Coal Geol.* 94, 3–21.
- Díaz, S.L., Espósito, M.E., del Carmen Blanco, M., Amiotti, N.M., Schmidt, E.S., Sequeira, M.E., Paoloni, J.D., Nicolli, H.B., 2016. Control factors of the spatial distribution of arsenic and other associated elements in loess soils and waters of the southern Pampa (Argentina). *Catena* 140, 205–216.
- DoE. (Department of Environment), 1997. Industrial Effluents Quality Standard for Bangladesh, Bangladesh Gazette Additional August, 28, 1997. The Environment Conservation Rules 1997. Government of the People's Republic of Bangladesh, Dhaka.
- Erarslan, C., Örgün, Y., Bozkurtoglu, E., 2014. Geochemistry of trace elements in the Keşan coal and its effect on the physicochemical features of ground- and surface waters in the coal fields, Edirne, Thrace Region, Turkey. *Int. J. Coal Geol.* 133, 1–12.
- Fallahzadeh, R.A., Ghaneian, M.T., Miri, M., Dashti, M.M., 2017. Spatial analysis and health risk assessment of heavy metals concentration in drinking water resources. *Environ. Sci. Pollut. Res.* 24 (32), 24790–24802.
- Finkelman, R.B., Orem, W.H., Plumlee, G.S., Selinus, O., 2018. Applications of geochemistry to medical geology (chapter 17). In: De Vivo, B., Blkin, H.E., Lima, A. (Eds.), In: *Environmental Geochemistry* (435–465), 2ndedn. Elsevier, Amsterdam, Netherlands.
- Frontasyeva, M.V., Pereygin, V.P., Vater, P. (Eds.), 2001. Radionuclides and Heavy Metals in Environment. Springer, Dordrecht. Dordrecht; London, p. 392 (Kluwer Academic Publishers).
- Galhardi, J.A., Bonotto, D.M., 2017. Radionuclides (^{222}Rn , ^{226}Ra , ^{234}U , and ^{238}U) release in natural waters affected by coal mining activities in Southern Brazil. *Water Air Soil Pollut.* 228 (6), 207.
- Geng, M., Qi, H., Liu, X., Gao, B., Yang, Z., Lu, W., Sun, R., 2016. Occurrence and health risk assessment of selected metals in drinking water from two typical remote areas in China. *Environ. Sci. Pollut. Res.* 23, 8462–8469.
- Habib, M.A., Basuki, T., Miyashita, S., Bekelesi, W., Nakashima, S., Techato, K., Khan, R., Majlis, A.B.K., Phoungthong, K., 2019. Assessment of natural radioactivity in coals and coal combustion residues from a coal-based thermoelectric plant in Bangladesh: implications for radiological health hazards. *Environ. Monit. Assess.* 191 (1), 27. <https://doi.org/10.1007/s10661-018-7160-y>.
- Habib, M.A., Basuki, T., Miyashita, S., Bekelesi, W., Nakashima, S., Phoungthong, K., Khan, R., Rashid, M.B., Islam, A.R.M.T., Techato, K., 2018. Distribution of naturally occurring radionuclides in soil around a coal-based power plant and their potential radiological risk assessment. *Radiochim. Acta.* <https://doi.org/10.1515/ract-2018-3044> (Accepted).
- Halim, M.A., Majumder, R.K., Zaman, M.N., Hossain, S., Rasul, M.G., Sasaki, K., 2013. Mobility and impact of trace metals in Barapukuria coal mining area, Northwest Bangladesh. *Arab J. Geosci.* 6 (12), 4593–4605.
- Haloi, N., Sarma, H.P., 2012. Heavy metal contaminations in the groundwater of Brahmaputra flood plain: an assessment of water quality in Barpeta District, Assam (India). *Environ. Monit. Assess.* 184 (10), 6229–6237.
- Hossain, M.N., Paul, S.K., Hasan, M.M., 2015. Environmental impacts of coal mine and thermal power plant to the surroundings of Barapukuria, Dinajpur, Bangladesh. *Environ. Monit. Assess.* 187 (4), 202.
- Howladar, M.F., Islam, M.R., 2016. A study on physico-chemical properties and uses of coal ash of Barapukuria coal-fired thermal power plant, Dinajpur, for environmental sustainability. *Energ. Ecol. Environ.* 1 (4), 233–247.
- He, S., Wu, J., 2018. Hydrogeochemical characteristics, groundwater quality and health risks from hexavalent chromium and nitrate in groundwater of Huanhe Formation in Wuqi County, northwest China. *Expo Health* 11 (2), 125–137. <https://doi.org/10.1007/s12403-018-0289-7>.
- He, X., Wu, J., He, S., 2019. Hydrochemical characteristics and quality evaluation of groundwater in terms of health risks in Luohe aquifer in Wuqi County of the Chinese Loess Plateau, northwest China. *Hum Ecol Risk Assess* 25 (1–2), 32–51. <https://doi.org/10.1080/10807039.2018.1531693>.
- Islam, A.R.M.T., Ahmed, N., Bodrud-Doza, M., Chu, R., 2017a. Characterizing groundwater quality ranks for drinking purposes in Sylhet district, Bangladesh, using entropy method, spatial autocorrelation index, and geostatistics. *Environ. Sci. Pollut. Res.* 24 (34), 26360–26374.
- Islam, A.R.M.T., Rakib, M.A., Islam, M.S., Jahan, K., Patwary, M.A., 2015. Assessment of health hazard of metal concentration in groundwater of Bangladesh. *Am. Chem. Sci. J.* 5 (1), 41–49.
- Islam, A.R.M.T., Shen, S., Bodrud-Doza, M., Rahman, M.A., Das, S., 2017b. Assessment of trace elements of groundwater and their spatial distribution in Rangpur district, Bangladesh. *Arab J. Geosci.* 10, 95.
- Islam, A.R.M.T., Shen, S., Bodrud-Doza, M., 2017c. Assessment of arsenic health risk and source apportionment of groundwater pollutants using multivariate statistical techniques in Chapai-Nawabganj district, Bangladesh. *J. Geol. Soc. India* 90, 239–248.
- Islam, M.A., Latif, S.A., Hossain, S.M., Uddin, M.S., Podder, J., 2011. The concentration and distribution of trace elements in coals and ashes of the Barapukuria thermal power plant, Bangladesh. *Energy Sources Part A* 33 (9), 898–898.
- Islam, A.R.M.T., Bodrud-doza, M., Rahman, M.S., Amin, S.B., Chu, R., Mamun, H.A., 2019. Sources of trace elements identification in drinking water of Rangpur district, Bangladesh and their potential health risk following multivariate techniques and Monte-Carlo simulation. *Groundwater for Sustainable Development* 9, 100275. <https://doi.org/10.1016/j.gsd.2019.100275>.
- Islam, M.R., Hayashi, D., 2008. Geology and coal bed methane resource potential of the Gondwana Barapukuria coal basin, Dinajpur, Bangladesh. *Int. J. Coal Geol.* 75 (3), 127–143.
- Ito, S., Yokoyama, T., Asakura, K., 2006. Emissions of mercury and other trace elements from coal-fired power plants in Japan. *Sci. Total Environ.* 368 (1), 397–402.
- Jelic, T.M., Estalilla, O.C., Sawyer-Kaplan, P.R., Plata, M.J., Powers, J.T., Emmett, M.,

- Kuentner, J.T., 2017. Coal mine dust desquamative chronic interstitial pneumonia: a precursor of dust-related diffuse fibrosis and of emphysema. *Int. J. Occup. Environ. Med.* 8 (3), 153–165.
- Karim, Z., 2011. Risk assessment of dissolved trace metals in drinking water of Karachi, Pakistan. *Bull. Environ. Contam. Toxicol.* 86, 676–678.
- Khan, H.R., Seddique, A.A., Rahman, A., Shimizu, Y., 2017. Heavy metals contamination assessment of water and soils in and around Barapukuria coal mine area, Bangladesh. *Am. J. Environ. Prot.* 6, 80–86.
- Kibria, G., Hossain, M.M., Mallick, D., Lau, T.C., Wu, R., 2016. Monitoring of metal pollution in waterways across Bangladesh and ecological and public health implications of pollution. *Chemosphere* 165, 1–9.
- Kumar, M., Ramanathan, A.L., AL, Tripathi, R., Farswan, S., Kumar, D., Bhattacharya, P., 2017. A study of trace element contamination using multivariate statistical techniques and health risk assessment in groundwater of Chhaprola Industrial Area, Gautam Buddha Nagar, Uttar Pradesh, India. *Chemosphere* 166, 135–145.
- Lu, S.Y., Zhang, H.M., Sojinu, S.O., Liu, G.H., Zhang, J.Q., Ni, H.G., 2015. Trace elements contamination and human health risk assessment in drinking water from Shenzhen, China. *Environ. Monit. Assess.* 187, 4220.
- Ma, F., Wan, Y., Yuan, G., Meng, L., Dong, Z., Hu, J., 2012. Occurrence and source of nitrosamines and secondary amines in groundwater and its adjacent Jialu River Basin, China. *Environ. Sci. Technol.* 46, 3236–3243.
- Majumder, R.K., Shimada, J., 2016. Hydrochemistry and environmental isotopes to identify the origin of Barapukuria coal mine inflow water, northwestern Bangladesh. *Austin J. Hydrol.* 3 (1), 1019, 2016.
- Neogi, B., Tiwari, A.K., Singh, A.K., Pathak, D.D., 2018. Evaluation of metal contamination and risk assessment to human health in a coal mine region of India: a case study of the North Karanpura coalfield. *Hum. Ecol. Risk Assess.* 1–13.
- Nephalama, A., Muzerengi, C., 2016. Assessment of the influence of coal mining on groundwater quality: case of Masisi village in the Limpopo province of South Africa. In: Drebenstedt, Carsten, Paul, Michael (Eds.), *Proceedings IMWA 2016*, Freiberg/Germany, pp. 430–438. *Mining Meets Water – Conflicts and Solutions*.
- Newman, C., Agioutantis, Z., Boede, G., Leon, J., 2017. Assessment of potential impacts to surface and subsurface water bodies due to longwall mining. *Int. J. Min. Sci. Technol.* 27, 57–64.
- Ochieng, G., Ochieng, G.M., Seanego, E.S., Nkwonta, O.I., 2015. Impacts of mining on water resources in South Africa: a review. *Sci. Res. Essays* 5, 3351–3357.
- Prasad, B., Kumari, S., 2008. Heavy metal pollution index of ground water of an abandoned opencast mine filled with fly ash. *Mine Water Environ.* 27 (4), 265–267.
- Qiu, H., Gui, H., Song, Q., 2018. Human health risk assessment of trace elements in shallow groundwater of the Linhuan coal-mining district, Northern Anhui Province, China. *Hum. Ecol. Risk Assess.* 7039, 1549–7860.
- Rahman, M.M., Islam, M.A., Bodrud-Doza, M., Muhib, M.I., Zahid, A., Shammi, M., Tareq, S.M., Kurasaki, M., 2018. Spatio-temporal assessment of groundwater quality and human health risk: a case study in Gopalganj. *Expo. Health* 10 (3), 167–188.
- Sengupta, D., Agrahari, S., 2017. Heavy metal and radionuclide contaminant migration in the vicinity of thermal power plants: monitoring, remediation, and utilization. In: *Modelling Trends in Solid and Hazardous Waste Management*. Springer, Singapore, pp. 15–33.
- Silva, L.F., de Vallejuelo, S.F.O., Martinez-Arkarazo, I., Castro, K., Oliveira, M.L., Sampaio, C.H., de Brum, I.A., de Leão, F.B., Taffarel, S.R., Madariaga, J.M., 2013. Study of environmental pollution and mineralogical characterization of sediment rivers from Brazilian coal mining acid drainage. *Sci. Total Environ.* 447, 169–178.
- Singh, A.K., Mahato, M.K., Neogi, B., Singh, K.K., 2010. Quality assessment of mine water in the Raniganj coalfield area, India. *Mine Water Environ.* 29, 248–262.
- Singh, R., Tajdarul, A.S.V., Reddy, H.S.A.G.S., Kumar, M., Kurakalva, R.M., 2017. Assessment of potentially toxic trace elements contamination in groundwater resources of the coal mining area of the Korba. *Environ. Earth Sci.* 76, 566.
- Singh, U.K., Ramanathan, A.L., Subramanian, V., 2018. Groundwater chemistry and human health risk assessment in the mining region of East Singhbhum, Jharkhand, India. *Chemosphere* 224, 501–513.
- Tiwari, A.K., Singh, P.K., Mahato, M.K., 2017. Assessment of metal contamination in the mine water of the West Bokaro Coalfield, India. *Mine Water Environ.* 36 (4), 532–541.
- US EPA, 1986. United States environmental Protection agency. Fed. Regist 51 (185), 34014–34025. http://www.epa.gov/oswer/riskassessment/human_health_toxicity.htm. (Accessed 8 May 2018).
- US EPA, 2004. Risk assessment guidance for superfund volume I: human health evaluation manual (part E). <http://www.epa.gov/oswer/riskassessment/rage/pdf/introduction.pdf>. (Accessed 10 September 2018).
- Voltaggio, M., Spadoni, M., Sacchi, E., Sanam, R., Pujari, P.R., Labhasetwar, P.K., 2015. Assessment of groundwater pollution from ash ponds using stable and unstable isotopes around the Koradi and Khaperkheda thermal power plants (Maharashtra, India). *Sci. Total Environ.* 518, 616–625.
- WHO. (World Health Organization), 2011. *Guideline for Drinking Water Quality*, fourth ed. World Health Organization (WHO), Geneva, Switzerland (World Health Organization).
- Wu, B., Zhao, D.Y., Jia, H.Y., Zhang, Y., Zhang, X.X., Cheng, S.P., 2009. Preliminary risk assessment of trace metal pollution in surface water from Yangtze River in Nanjing Section, China. *Bull. Environ. Contam. Toxicol.* 82, 405–409.
- Yang, M., Fei, Y., Ju, Y., M, Z., Li, H., 2012. Health risk assessment of groundwater pollution—a case study of typical city in North China Plain. *Jour. Earth Sci.* 23 (3), 335–348.
- Zaman, R., Bruderermann, T., Kumar, S., Islam, N., 2018. A multi-criteria analysis of coal-based power generation in Bangladesh. *Energy Policy* 116, 182–192.
- Zeng, B., Zhang, Z., Yang, M., 2018. Risk assessment of groundwater with multi-source pollution by a long-term monitoring programme for a large mining area. *Int. Biodeterior. Biodegrad.* 128, 100–108.
- Zhang, S., Liu, G., Sun, R., Wu, D., 2016. Health risk assessment of heavy metals in groundwater of coal mining area: a case study in Dingji coal mine, Huainan Coalfield, China. *Hum. Ecol. Risk Assess.* 22 (7), 1469–1479.